In: Mathematical Methods and Models
Editor: Alain Miranville, pp. 43-77

ISBN 1-59454-317-8
©2005 Nova Science Publishers, Inc.

Chapter 2

MECHANICAL EFFECTS IN THE CAHN-HILLIARD MODEL: A REVIEW ON MATHEMATICAL RESULTS

Harald Garcke
Universtät Regensburg

Abstract

We review mathematical results on the Cahn-Hilliard equation with elasticity (the Cahn-Larché system). Pattern formation during spinodal decomposition is discussed as well as existence and uniqueness results. Furthermore, the relation of the Cahn-Hilliard equation to a sharp interface model (a modified Mullins-Sekerka problem) is studied. Recent applications of a degenerate Cahn-Larché system to model surface diffusion in the presence of elastic interactions are outlined. Finally, a finite element method to numerically approximate solutions of the Cahn-Larché system is presented.

1 Introduction

The Cahn-Hilliard model was introduced [13, 15] to describe spinodal decomposition, i.e. the demixing of a homogeneous alloy which is quenched under its critical temperature θ_c. Above the critical temperature the homogeneous state (i.e. a constant concentration of the alloy components) is stable, but cooled underneath its critical temperature this state becomes unstable and the system locally tends to decompose into two or more phases. Later it was noticed that the Cahn-Hilliard equation also describes the rearrangement of phase boundaries after regions of different phases have been formed. This has been shown with the help of numerical simulations (see e.g. Elliott [27] and the references therein) and by formally matched asymptotic expansions (see Pego [72]). Also the coarsening of particles, i.e. regions occupied by the same phase, can be modelled by the Cahn-Hilliard equation (see [53] and [41]). This process is called Ostwald ripening.

The original Cahn-Hilliard model takes the chemical free energy and energy contributions due to capillary effects into account. But also mechanical effects can have a pronounced influence on both the process of spinodal decomposition and on the movement of

phase boundaries. In particular the shape of the phase boundaries will change and if the elasticity tensor in the two phases is different, the coarsening process can either accelerate, slow down or even stop (see [35]).

In this paper we consider the case of a binary alloy, i.e. two alloy components are present (for the treatment of multi-component alloys see [37, 38]). Denoting by c_1 and c_2 the concentrations of the components we will use the concentration difference $c = c_1 - c_2$ as variable which determines the concentrations due to the constraint $c_1 + c_2 = 1$. As second unknown field we introduce the displacement vector $u(t,x)$, which describes that a point x in the reference configuration will be at the point $x + u(t,x)$ at time t. The linearized strain tensor is given by

$$\mathcal{E}(u) = \tfrac{1}{2}(\nabla u + (\nabla u)^T)$$

where ∇ is the spatial gradient and $(\nabla u)^T$ is the transpose of ∇u. The free energy of the system is then given by

$$E(c,u) = \int_\Omega \left\{ \tfrac{\gamma}{2}|\nabla c|^2 + \psi(c) + W(c, \mathcal{E}(u)) \right\} dx$$

where $\Omega \subset \mathbb{R}^d$ is the region under consideration, $\gamma > 0$ is a small interfacial parameter, $\psi : \mathbb{R} \to \mathbb{R}$ is the non-convex free energy density and $W : \mathbb{R} \times \mathbb{R}^{d\times d} \to \mathbb{R}$ is the elastic energy density. A homogeneous free energy density ψ for a mean field model at a fixed absolute temperature is

$$\psi(c) = \tfrac{R\theta}{2}\{(1+c)ln(1+c) + (1-c)ln(1-c)\} + \tfrac{R\theta_c}{2}(1-c^2). \tag{1}$$

Here θ_c is the critical temperature and R is the gas constant scaled by the (constant) molar volume. For θ below the critical temperature θ_c the energy density ψ has two global minima c_-, c_+ and hence a non-convex form. Two approximations to ψ are frequently used. For shallow quenches, i.e. $0 << \theta < \theta_c$ one takes the quartic polynomial

$$\psi(c) = b(c^2 - a^2)^2 \,,\ 0 < a < 1, b > 0 \tag{2}$$

and for deep quenches, i.e. θ close to zero the double obstacle potential

$$\psi(c) = \begin{cases} \frac{R\theta_c}{2}(1-c^2) & \text{if} \quad |c| \le 1\,, \\ \infty & \text{elsewhere} \end{cases} \tag{3}$$

has been suggested by Blowey and Elliott [8].

The elastic energy density is usually taken to be a quadratic function of $\mathcal{E}$ and introducing the stress free strains (or eigenstrains) $\overline{\mathcal{E}}(c)$ we write

$$W(c, \mathcal{E}) = \tfrac{1}{2}(\mathcal{E} - \overline{\mathcal{E}}(c)) : C(c)(\mathcal{E} - \overline{\mathcal{E}}(c)). \tag{4}$$

$C(c)$ is the fourth rank elasticity tensor and the :–product is the inner product between linear mappings, i.e. $A : B = tr(A^T B)$ for mappings A and B (here tr denotes the trace of a mapping). The elasticity tensor C is assumed to be symmetric and positive definite which

implies that W is zero, if and only if $\mathcal{E} = \overline{\mathcal{E}}(c)$ meaning that for a concentration c the strain $\overline{\mathcal{E}}(c)$ is the energetically favourable strain. For $\overline{\mathcal{E}}$ usually an affine linear ansatz (Vegard's law) is used, i.e.

$$\overline{\mathcal{E}}(c) = \widehat{\mathcal{E}} + \mathcal{E}^* c,$$

where $\widehat{\mathcal{E}}, \mathcal{E}^* \in \mathbb{R}^{d\times d}$ are symmetric. The eigenstrains describe e.g. the elastic misfit between the two alloy components. In general the elasticity tensor can be different for the alloy components and therefore we allow for a c–dependence of the elasticity tensor C. For an isotropic material we obtain

$$C(c)\mathcal{E} = 2\mu(c)\mathcal{E} + \lambda(c)tr(\mathcal{E})Id$$

where the Lamé moduli μ and λ depend on the concentration c.

For a material with cubic symmetry we have

$$C(c)\mathcal{E} = 2\mu(c)\mathcal{E} + \lambda(c)tr\mathcal{E}Id + \mu'(c)\operatorname{diag}\mathcal{E}$$

where $\operatorname{diag}\mathcal{E}$ is the matrix that you obtain, if you set all off-diagonal entries to zero. In general C is an arbitrary fourth rank tensor $C(c) = (C_{ijl'j'}(c))$ and using the symmetry conditions

$$C_{ijl'j'} = C_{ijj'l'} = C_{jil'j'} = C_{l'j'ij}$$

one can compute that for $d = 3$ there are 21 degrees of freedom in C which of course in general will be restricted by crystal symmetry.

For example in a cubic system we obtain that $C_{1111} = C_{2222} = C_{3333}$, $C_{iijj} = C_{ii\kappa\kappa}$ (for i, j, κ mutually different), $C_{2323} = C_{3131} = C_{1212}$ and all other entries in C either follow from the above by symmetry or they are zero. Sometimes a fourth rank tensor in $\mathbb{R}^3$ is denoted by C_{ij} (Voigt notation). In this case the indices i, j take values $1,2,3,4,5,6$ and they stand for the pairs $11, 22, 33, 23, 31, 12$ in the original notation. This means in a cubic system we only need to specify C_{11}, C_{12} and C_{44}. All other parameters are determined as above. For a discussion of other symmetry classes we refer to Gurtin [48]. We will also always assume that $C(c)$ is positive definite and bounded uniformly in c.

Taking mechanical effects in the Cahn-Hilliard model into account we obtain the system

$$\partial_t c = \nabla \cdot (b\nabla w), \tag{5}$$

$$w = \frac{\delta E}{\delta c} = -\gamma\Delta c + \psi'(c) + W_{,c}(c, \mathcal{E}(u)), \tag{6}$$

$$0 = \frac{\delta E}{\delta u} = -\nabla \cdot W_{,\mathcal{E}}(c, \mathcal{E}(u)), \tag{7}$$

which we sometimes also call the Cahn-Larché system (see [16, 55]). Here $\frac{\delta E}{\delta c}$ denotes the first variation of E with respect to c and $W_{,c}$ is the partial derivative with respect to c (the same notation holds with respect to u). Furthermore, b is the nonnegative mobility coefficient which in general can depend on the concentration c. In Sections 2, 3 and 6 for the ease of presentation we will set $b \equiv 1$. The chemical potential w is the diffusion

potential and is given by the first variation of energy with respect to concentration. The quantity $S = W_{,\mathcal{E}}$ is the stress and hence (7) are the mechanical equilibrium equations from the theory of elasticity.

The set of equations then has to be completed by appropriate boundary conditions which can be e.g. periodic boundary conditions or Neumann boundary conditions for w and c and a prescribed normal stress at the boundary for the u–equation.

For the system (5)-(7) an appropriate formulation of the second law of thermodynamics holds. For isothermal systems the second law can be stated as a dissipation inequality for the free energy. And in fact one computes that the following inequality holds

$$\partial_t(\tfrac{\gamma}{2}|\nabla c|^2 + \psi(c) + W(c,\mathcal{E})) \leq \nabla \cdot (\gamma \nabla c\, \partial_t c + S\partial_t u - Jw) \tag{8}$$

where $J = -b\nabla w$ is the mass flux. Hence the increase of free energy does not exceed the total power expended plus the energy inflow which is an appropriate form of the second law (see [37, 38] for more details). For appropriate boundary conditions the free energy inequality (8) will give important a priori estimates (see Section 3).

In the forthcoming sections we will review mathematical results on the Cahn-Larché equation obtained by the author in recent years, some in collaboration with colleagues which will be mentioned in the text. First we will discuss the influence of elastic effects on spinodal decomposition which is the process in which after quenching below the critical temperature different phases form. We will see later in Section 2 that the morphology that develops will depend crucially on the elastic properties of the materials.

In Section 3 we will present existence and uniqueness results for the Cahn-Hilliard equation. Here we will make use of the gradient flow structure of the system. The Cahn-Hilliard equation is a diffuse interface model, i.e. interfaces between regions of different phases are modelled by an interfacial layer across which the physical fields vary continuously. At later stages in the evolution when regions consisting of different phases have been formed the rearrangements of these regions can also be described by a sharp interface model, i.e. phases are separated by hypersurfaces across which some fields may jump. The relation of the Cahn-Larché model to a sharp interface model will be discussed in Section 4.

In Section 5 we will discuss a recent application of the Cahn-Larché equation with degenerate mobility as a model for surface diffusion in the presence of elastic interactions. This model has important applications, e.g. void migration in microelectronic interconnects can be described with the help of this approach. Finally, we will briefly discuss approaches to numerically solve the Cahn-Larché system.

The presentation in this paper is rather informal. We will not always state results and proofs with full rigour but we will always refer to the literature for the complete statement of theorems and proofs.

2 Spinodal Decomposition

In this section we consider the phase separation process. We consider initial conditions for the concentrations which are slight perturbations of a homogeneous unstable state. This is the situation one encounters in applications when a formerly stable homogeneous state is quenched underneath its critical temperature θ_c. The state then can become unstable and in this case phases form which are distinguished from each other by a different chemical concentration. Typically the phases form regions of small diameters and a microstructure consisting of many regions form. If the elasticity tensor or the eigenstrains are anisotropic, one will observe that the phase boundaries will predominantly align with certain directions (see e.g. [40, 42]). It is the goal of this section to analyze this phenomenon and to understand why certain patterns form. We will do this with the help of a linearized stability analysis for the Cahn-Larché equation around a homogeneous state. We will also state a theorem (see [40]) which roughly says that we will see certain patterns with a probability close to one.

In our analysis we will solve linearized equations with the help of the Fourier transformation. Therefore we consider periodic boundary conditions and study a rectangular domain

$$\Omega = (0, 2\pi) \times \cdots \times (0, 2\pi).$$

We also assume that

$$\overline{\mathcal{E}}(c) = \mathcal{E}^* c$$

which just means that we choose a reference state in which the two components have equal concentration. Furthermore, we only consider the case of homogeneous elasticity, i.e. C does not depend on the concentration c. If we linearize the Cahn-Larché system around a constant stationary state $(c, u) = (c_m, 0)$, we obtain (we also denote the linearized variable in the concentration equation by c)

$$\begin{aligned} \partial_t c &= (-\Delta)(\gamma \Delta c - \psi''(c_m)c + \mathcal{E}^* : S), && (9)\\ 0 &= \nabla \cdot S, && (10)\\ S &= C[\mathcal{E}(u) - \mathcal{E}^* c]. && (11) \end{aligned}$$

We can now eliminate u in the equation for the concentration, if we introduce an operator $\mathcal{L}$ by

$$\begin{aligned} \mathcal{L} \;:\; X &\to X, \\ c &\mapsto \mathcal{E}^* : S \end{aligned}$$

where

$$X := \{c \in L^2(\Omega) \mid \int_\Omega c\,dx = 0\}$$

and S is given by a solution of (10), (11) with periodic boundary conditions. Hence (9) can be written as

$$\partial_t c = (-\Delta)(\gamma \Delta c - \psi''(c_m)c + \mathcal{L}(c)). \qquad (12)$$

The operator $\mathcal{L}(c)$ can be computed by Fourier transformation. For the Fourier mode

$$\varphi_\kappa(x) = e^{\mathbf{i}\kappa\cdot x}, \quad \mathbf{i} \text{ being the imaginary unit,}$$

with

$$\kappa = (\kappa_1, \ldots, \kappa_d) \in \mathbb{Z}^d$$

one obtains (see [52, 40])

$$\mathcal{L}(\varphi_\kappa) = L(\kappa)\varphi_\kappa$$

where

$$L(\kappa) = \mathcal{E}^* : (C[Z(\kappa)S^*\kappa\kappa^T] - S^*)$$

where $S^* := C[\mathcal{E}^*]$ and $Z(\kappa)$ is the inverse of

$$Z^{-1}(\kappa) = \left(\sum_{j,m}^{d} C_{ijmn}\kappa_j\kappa_m \right)_{i,n=1,\ldots,d}.$$

An important observation is that L is homogeneous of degree 0 which implies that $\mathcal{L}$ is a pseudo-differential operator of order 0. The function L can be computed more explicitely in certain cases, e.g. if C is isotropic or has a cubic symmetry (see [40]). In the particular case of cubic symmetry one obtains that certain directions $\kappa \in \mathbf{Z}^d$ are stronger amplified by L than others. This has important consequences for (12). If we consider solutions to (12) of the separation of variables form

$$c(x,t) = f(t)e^{\mathbf{i}\kappa\cdot x},$$

we obtain

$$f(t) = \alpha e^{\lambda_{\kappa,\gamma}t}, \alpha \in \mathbb{R},$$

with

$$\lambda_{\kappa,\gamma} = |\kappa|^2(-\gamma|\kappa|^2 - \psi''(c_m) + L(\kappa)).$$

If c_m is such that $\psi''(c_m) < 0$, one obtains in the case without elasticity that all κ with a certain wave length are amplified the most. Now in case of anisotropic elasticity also the direction of κ plays an important role when we want to determine the most unstable waves. It turns out (see [16, 40] and the references therein) that in case of cubic anisotropy either directions parallel to the coordinate axes or direction parallel to the diagonals of the coordinate axes are amplified more by the influence of elastic interactions. Which of the two cases occur depends on the parameter $\Delta C := C_{11} - C_{12} - 2C_{44}$. One speaks of positive anisotropy if $\Delta C > 0$ and of negative anisotropy if $\Delta C < 0$. We demonstrate the effect of different ΔC's in the Figures 1, 2 and 3. In all figures we show on the left with dark colour which Fourier modes in the (κ_1, κ_2)–plane are amplified the most. We see for example that in the isotropic case no directions are preferred. This is as in the case of the Cahn-Hilliard equation, i.e. in the case that no elastic effects are incorporated. In case of cubic elasticity either the coordinate axes (in case of negative anisotropy) or the diagonals (in case of positive anisotropy) and here only modes with certain wave lenghts are amplified the most.

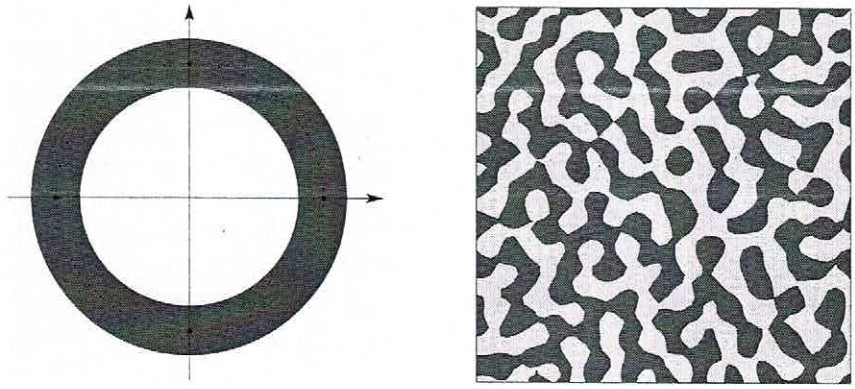

Figure 1: The most amplified eigenmodes (left) and a typical pattern (right) for isotropic elasticity ($\Delta C = 0$)

Using methods developed by Maier-Paape and Wanner [63] it is shown by Garcke, Maier-Paape and Weikard [40] that with a probability close to one, the dynamics of randomly chosen initial data in the neighborhood of a uniform mixture will be dominated by an invariant manifold which is tangential to the most unstable eigenfunctions of the linearized operator. For a precise statement of the result see [40]. For example in the case of cubic anisotropy it was shown that the most unstable eigenfunctions reflect the cubic anisotropy and therefore, the anisotropy will influence the dynamics quite drastically. This shows in particular that elastic effects are not only important at later stages of the evolution, but they also determine the morphology after spinodal decomposition (see Figures 4, 5 for numerical solutions of the Cahn-Larché system).

3 Existence and Uniqueness Results

3.1 The Gradient Flow Structure

In case that the elasticity tensor depends on the concentration c (this is called the case of inhomogeneous elasticity) the mathematical analysis for (5)-(7) becomes sophisticated, because a term quadratic in ∇u enters the equation for the chemical potential: Existence and uniqueness results for different variants of the system (5)-(7) have been given independently by Carrive, Miranville and Piétrus [18], Bonetti et al. [10] and Garcke [37, 38]. In this review we will shortly discuss the results of [37, 38] which obtains results for (5)-(7) with the boundary conditions

$$\nabla c \cdot n = 0\,, \nabla w \cdot n = 0\,, Sn = 0 \tag{13}$$

where n is the outer unit normal to Ω.

The approach to show existence in [37] is based on an implicit time discretization of (5)-(7) and uses the fact that (5)-(7) can be interpreted as a gradient flow. To make this

Univ.-Bibliothek Regensburg

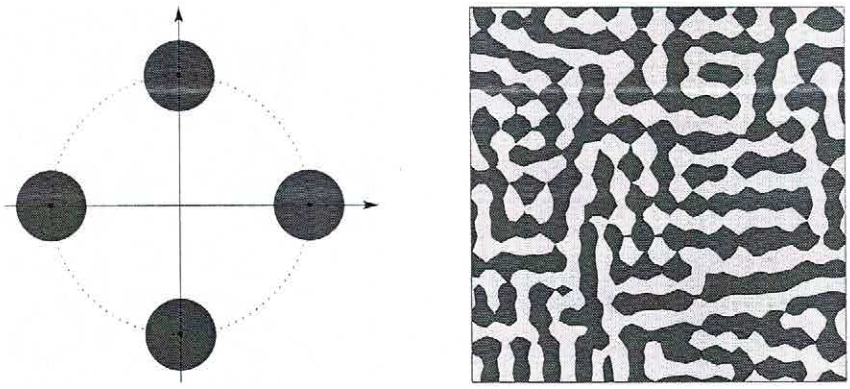

Figure 2: The most amplified eigenmodes (left) and a typical pattern (right) for negative anisotropy ($\Delta C < 0$)

precise we need to introduce the H^{-1}-scalar product. We define the spaces

$$\mathcal{Y} = \{z \in H^1(\Omega) \mid \int_\Omega z = 0\}$$

and

$$\mathcal{D} = \{f \in (H^1(\Omega))^* \mid \langle 1, f\rangle = 0\}$$

where $(H^1(\Omega))^*$ is the dual space of $H^1(\Omega)$ and $\langle\cdot,\cdot\rangle$ is the duality pairing between $H^1(\Omega)$ and $(H^1(\Omega))^*$. Now the Green's operator $\mathcal{G}$ (or the inverse negative Laplacian operator) for $(-\Delta)$ with Neumann boundary condition is defined via

$$\begin{aligned} \mathcal{G} \quad : \quad & \mathcal{D} \to \mathcal{Y} \\ & f \mapsto \mathcal{G}f \end{aligned}$$

where $\mathcal{G}f$ fulfills

$$(\nabla \mathcal{G}f, \nabla\zeta)_{L^2} = \langle \zeta, f\rangle$$

for all $\zeta \in H^1(\Omega)$. Now the H^{-1}-scalar product is given by

$$(f_1, f_2)_{-1} := (\nabla \mathcal{G}f_1, \nabla \mathcal{G}f_2)_{L^2} \quad \text{for all} \quad f_1, f_2 \in \mathcal{D}.$$

Now it follows that the equations (5), (6) can formally be reformulated as

$$\left\langle \zeta, \frac{\delta E}{\delta c} \right\rangle = -(\zeta, \partial_t c)_{-1} \quad \text{for all} \quad \zeta \in \mathcal{Y}. \tag{14}$$

Let us shortly review the concept of gradient flows. For a functional E on a space X and an inner product $(\cdot,\cdot)_X$ on X we say that a time dependent function c with values in X is a solution of the gradient flow equation to E and $(\cdot,\cdot)_X$ if and only if

$$\left\langle \zeta, \frac{\delta E}{\delta c} \right\rangle = -(\zeta, \partial_t c)_X \quad \text{for all} \quad \zeta \in Y,$$

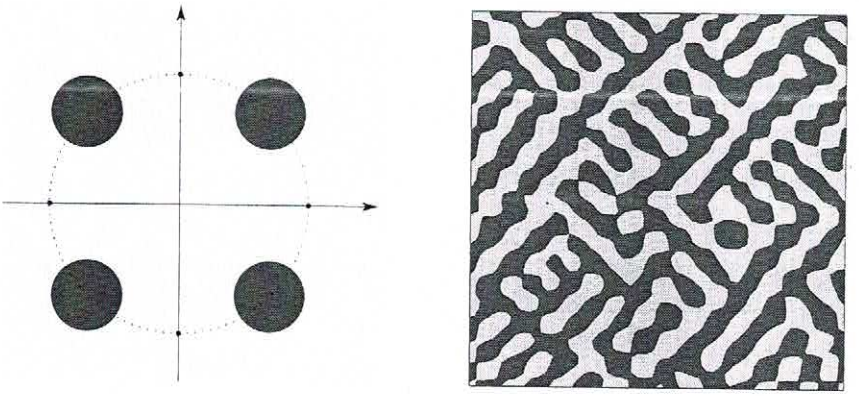

Figure 3: The most amplified eigenmodes (left) and a typical pattern (right) for positiv anisotropy ($\Delta C > 0$)

where Y is a dense subspace of X. Hence, (14) shows that the equation (5), (6) realize the gradient flow of E in the H^{-1}-scalar product (with respect to the variable c).

3.2 Existence for Smooth Potentials

The aim of [37, 38] was to show existence of weak solutions to (5)-(7) by using the gradient flow structure of the evolution. In fact the following result was shown in [37, 38].

Theorem 3.1 *Assume $\Omega \subset \mathbb{R}^d$ is a bounded domain with Lipschitz boundary, ψ is of the form (2), W is of the form (4) and a $c^0 \in H^1(\Omega)$ is given such that $\int_\Omega \psi(c^0) < \infty$.*

Then there exists a weak solution of (5)-(7) with the properties

(i) $c \in C^{0,\frac{1}{4}}([0,T];L^2(\Omega))$,

(ii) $\partial_t c \in L^2(0,T;(H^1(\Omega))^*)$,

(iii) $u \in L^\infty(0,T,H^1(\Omega,\mathbb{R}^n))$,

(iv) $c(0) = c^0$.

Remark 3.1 *For a precise definition of weak solution and for more general assumptions for which the theorem is true we refer to [37, 38].*

We will not give a detailed proof of the theorem. Instead we will outline the main ideas. The proof uses an implicit time discretization of (5)-(7) to obtain approximate solutions. Existence of solutions to the time-discrete problem can be shown with the help of the direct method of the calculus of variations. Here, it is important to use the gradient flow structure of the problem in order to obtain that the time discrete problem is the Euler-Lagrange equation of a certain functional.

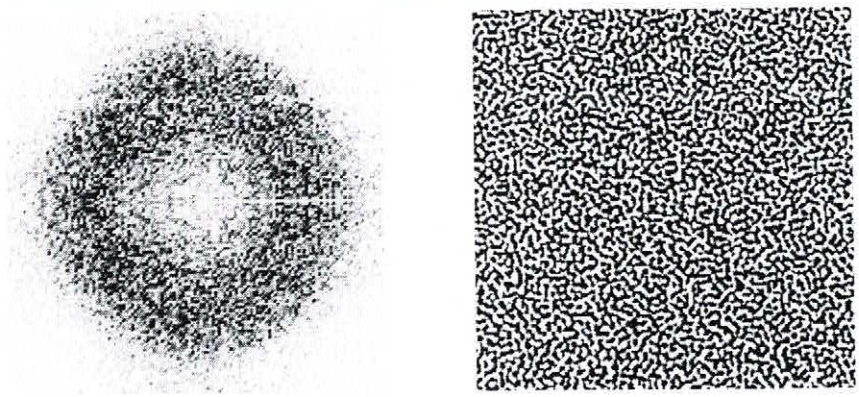

Figure 4: Patterns after spinodal decomposition without elasticity; modulus of the Fourier coefficient (left) and sign of the concentration difference c (right). If one includes homogeneous elasticity the patterns are similar.

Using the gradient flow property we obtain natural a priori estimates from the fact that the free energy E is a Lyapunov functional. The remaining part of the proof then uses compactness arguments in order to pass to the limit in the time-discrete problem. For the detailed proof we refer to [37, 38]. Here we only briefly discuss the implicit time discretization and the use of the gradient flow structure.

The implicit time discretization (the backward Euler scheme) for (5)-(7) can be written in the weak form

$$\left\langle \zeta, \frac{\delta E}{\delta c}(c^m, u^m) \right\rangle = -\left(\zeta, \frac{c^m - c^{m-1}}{\Delta t} \right)_{-1} \quad \text{for all } \zeta \in \mathcal{Y}, \tag{15}$$

$$\left\langle \eta, \frac{\delta E}{\delta u}(c^m, u^m) \right\rangle = 0 \quad \text{for all} \quad \eta \in H^1(\Omega, \mathbb{R}^d). \tag{16}$$

It can be verified that the above two identities are the Euler-Lagrange equations of the functional

$$E^{m,\Delta t}(d,v) := E(d,v) + \tfrac{1}{2\Delta t}\|d - c^{m-1}\|_{-1}^2.$$

The goal now is to minimize $E^{m,\Delta t}$ on the set $X^0 \times X_{\text{ird}}^{\perp}$, where

$$X^0 := \{c \in H^1(\Omega) \mid \int_\Omega c = \int_\Omega c^0\},$$

$$X_{\text{ird}} := \{u \in H^1(\Omega, \mathbb{R}^d) \mid \text{there exist } b \in \mathbb{R}^d \text{ and a skew symmetric } A \in \mathbb{R}^{d\times d} \text{ such that } u(x) = b + Ax\},$$

and $X_{\text{ird}}^{\perp}$ is the space perpendicular to X_{ird}.

We start with $m = 1$ which corresponds to the time Δt and then solve iteratively for $m = 2, 3, \ldots$ to obtain time discrete solutions, which we choose as absolute minimizers of $E^{m,\Delta t}$, at times $2\Delta t, 3\Delta t, \ldots$.

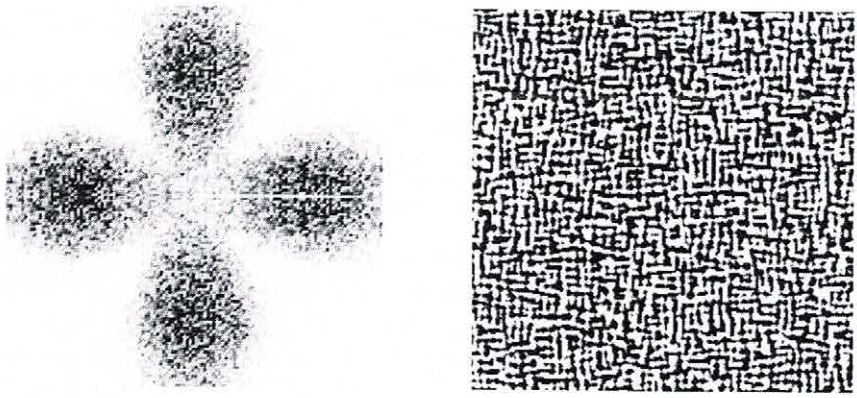

Figure 5: Cubic anisotropy of the elasticity tensor; modulus of the Fourier coefficient (left) and sign of the concentration difference c. (right)

The existence of an absolute minimizer follows by the direct method of calculus of variations where we obtain coercivity with the help of the inequalities of Korn and Poincaré.

As mentioned above an absolute minimizer of $E^{m,\Delta t}$ fulfills the Euler-Lagrange equations (15) and (16). Now we define

$$w^m = \mathcal{G}\left(\frac{c^m - c^{m-1}}{\Delta t}\right) + \lambda^m \tag{17}$$

where

$$\lambda^m = \tfrac{1}{|\Omega|}\int_\Omega \{\psi'(c^m) + W_{,c}(c^m, \mathcal{E}(u^m))\}$$

is a constant Lagrange multiplier. Now (5)-(7) give that the discrete solutions are solutions of the implicit time discretization of (5)-(7).

We denote by $(c^m_{\Delta t}, w^m_{\Delta t}, u^m_{\Delta t})$ the solution at time $m\Delta t$ that we obtain by solving the implicit time discretization with time step Δt. Then by taking $(c^{m-1}_{\Delta t}, u^{m-1}_{\Delta t})$ as a comparison function when minimizing $E^{m,\Delta t}$ we obtain

$$E(c^m_{\Delta t}, u^m_{\Delta t}) + \tfrac{1}{2\Delta t}\|c^m_{\Delta t} - c^{m-1}_{\Delta t}\|^2_{-1} \le E(c^{m-1}_{\Delta t}, u^{m-1}_{\Delta t}).$$

Using this inequality iteratively and using the definition of $w^m_{\Delta t}$ (which we extend to a function $w_{\Delta t}$ that is defined for all t by piecewise constant extension) we obtain

$$E(c^m_{\Delta t}, u^m_{\Delta t}) + \tfrac{1}{2}\int_0^{m\Delta t} |\nabla w_{\Delta t}|^2 \le E(c^0, u^0).$$

This is the main a priori estimate needed in order to pass to the limit $\Delta t \to 0$. One important step is to show strong convergence of ∇u in $L^2(\Omega_T)$ in order to pass to the limit in the term $W_{,c}$ appearing in the equation for the chemical potential w. We point out that in the case of inhomogeneous elasticity $W_{,c}$ contains quadratic terms in ∇u. How to handle this and how to pass to the limit in the discrete equations in order to show that limits of the discrete solutions solve (5)-(7) is shown in [37, 38].

3.3 Existence for Logarithmic Potentials

If the free energy density ψ is given by the logarithmic form (1) the mathematical analysis becomes more involved. Then the equation for the chemical potential reads

$$w = -\gamma\Delta c + \tfrac{R\theta}{2}(\ln(1+c) - \ln(1-c)) - R\theta_c c + W_{,c}(c, \mathcal{E}(u)) \tag{18}$$

which means that the equation for the chemical potential contains a term that becomes singular if $c \to \pm 1$. On the other hand this term guarantees already in the Cahn-Hilliard equation without elasticity that the solution remains between -1 and 1 which is the range of values that are physically meaningful (see [31]). If one chooses a smooth potential like in Subsection 3.2 this is not guaranteed due to the lack of a maximum principle for parabolic equations of fourth order.

In the case without elasticity one can use the convexity of the logarithmic term in ψ in order to get enough information on the logarithmic term in (18) for an existence result (see [31]). In the case with elasticity this is not so easy. The term $W_{,c}(c, \mathcal{E}(u))$, stemming from the elastic part of the energy, contains quadratic terms in ∇u and hence this term is controlled only in $L^1(\Omega_T)$. This is not enough to get good control on the logarithmic term. As often, L^1-control of a term is critical and we need only a little bit more information to proceed. This can be achieved by showing first a higher integrability result on ∇u by extending results of Giaquinta and Modica [45] to elasticity systems. Here we also need to extend the local results of [45] to a global version, i.e. we also need to derive estimates at the boundary. To be a bit more precise:

There exists a $p > 2$ not depending on c such that solutions to (7) fulfill

$$\nabla u(t) \in L^p(\Omega, R^{d\times d})$$

and

$$\|\nabla u(t)\|_{L^p(\Omega,\mathbb{R}^{d\times d})} \leq \tilde{c}(\|\nabla u(t)\|_{L^2(\Omega,\mathbb{R}^{d\times d})} + \|c(t)\|_{L^p(\Omega)} + 1)$$

where $\tilde{c}$ does not depend on c.

This result is then a basic ingredient to show the following existence result.

Theorem 3.2 *Let the assumptions of Theorem 3.1 hold but with ψ of the form (1). Furthermore we assume that $\fint c_0 \in (-1, 1)$.*

Then there exists a weak solution of (5)-(7) with the properties

(i) $c \in C^{0,\frac{1}{4}}([0,T], L^2(\Omega))$,

(ii) $\partial_t c \in L^2(0,T; (H^1(\Omega))^*)$,

(iii) $u \in L^\infty(0,T; W^{1,p}(\Omega, \mathbb{R}^d))$,

(iv) $c(0) = c^0$,

(v) there exists a $q > 1$ such that $\ln(1+c)$, $\ln(1-c) \in L^q(\Omega_T)$.

In particular, $c \in (-1,1)$ *almost everywhere.*

The theorem is proved with the help of approximation problems in which we modify ψ by smooth functions, a priori estimates (in particular using the higher integrability of ∇u), compactness results and passing to the limit in the regularized problem. To show (v) it is crucial that the logarithmic singularity in ψ is convex. For details we refer to [37, 39].

3.4 Uniqueness for Homogeneous Elasticity

One speaks of homogeneous elasticity, if the elasticity tensor C does not depend on the concentration c. In this case it is possible to show uniqueness. Let us briefly outline formally how this is possible. Here again the H^{-1} gradient flow structure will be used.

Let us assume there are two solutions (c_1, w_1, u_1) and (c_2, w_2, u_2) of (5)-(7) that fulfill the boundary conditions (13). Then we compute, using properties of the H^{-1} scalar product derived in Subsection 3.1 and the fact $\mathcal{G}\partial_t(c_1 - c_2) = -(w_1 - w_2)$

$$\begin{aligned}
\frac{d}{dt}\tfrac{1}{2}\|c_2 - c_1\|_{-1}^2 &= (c_2 - c_1, \partial_t(c_2 - c_1))_{-1} \\
&= (\nabla\mathcal{G}(c_2 - c_1), \nabla\mathcal{G}(\partial_t(c_2 - c_1)))_{L^2} \\
&= (c_2 - c_1, \mathcal{G}\partial_t(c_2 - c_1))_{L^2} \\
&= -((c_2 - c_1, w_2 - w_1)_{L^2} \\
&= -\|\nabla(c_2 - c_1)\|_{L^2}^2 - \int_\Omega (\psi'(c_2) - \psi'(c_1))(c_2 - c_1) \\
&\quad - \int_\Omega \mathcal{E}((u_2 - u_1) - \overline{\mathcal{E}}(c_2 - c_1)) : C(\mathcal{E}(u_2 - u_1) - \overline{\mathcal{E}}(c_2 - c_1))
\end{aligned}$$

where we used the mechanical equilibrium (7) and the linearity of $W_{,c}$ and $W_{,\mathcal{E}}$ to obtain the last identity. Now we can use the fact that for the homogeneous free energy densities (1) or (2) the inequality

$$(\psi'(c_2) - \psi'(c_1))(c_2 - c_1) \geq -c_\psi |c_2 - c_1|^2$$

holds, to obtain for $\overline{c} := c_2 - c_1$ und $\overline{u} := u_2 - u_1$

$$\|\overline{c}\|_{-1}(t) + \int_0^t \|\nabla\overline{c}\|_{L^2}^2 + \int_{\Omega_t} (\mathcal{E}(\overline{u}) - \overline{\mathcal{E}}(\overline{c})) : C(\mathcal{E}(\overline{u}) - \overline{\mathcal{E}}(\overline{c})) \leq c_\psi \int_0^t \|\overline{c}\|_{L^2}^2.$$

Since

$$\begin{aligned}
\|\overline{c}\|_{L^2}^2 &= (\nabla\mathcal{G}\overline{c}, \nabla\overline{c})_{L^2} \\
&\leq \|\nabla\mathcal{G}\overline{c}\|_{L^2}\|\nabla\overline{c}\|_{L^2} \\
&\leq \tfrac{1}{\delta}\|\overline{c}\|_{-1}^2 + \delta\|\nabla\overline{c}\|_{L^2}^2
\end{aligned}$$

we obtain $\overline{c} \equiv 0$ with the help of Gronwall's inequality.

In [37, 38] this argument has been made rigorous and one obtains

Theorem 3.3 *Assume $\Omega \subset \mathbb{R}^d$ is a bounded domain with Lipschitz boundary, ψ is either of the form (1) or (2), W is of the form (4) where C does not depend on c.*

Then there exists a unique weak solution of (5)-(7), (13) for given initial data $c^0 \in H^1(\Omega)$.

Remark 3.2 *For the above theorem to hold c^0 has to fulfill $\int_\Omega \psi(c^0) < \infty$ in the case that ψ is of the form (4) and $-1 < \fint c^0 < 1$ in the case that ψ is of the form (2).*

Remark 3.3 *i) Uniqueness in the case of inhomogeneous elasticity is not known so far.*
ii) Precise regularity results for the Cahn-Larché-system are not known. Bootstrap arguments are difficult at least in the case of inhomogeneous elasticity. This is due to the quadratic term $W_{,\mathcal{E}}$ in the w-equation.

4 The Sharp Interface Limit

4.1 The Γ-Limit of the Free Energy

In the Cahn-Hilliard and Cahn-Larché models the interface is diffuse, i.e. phases are separated by a thin diffusional layer. We now study the sharp interface limit, i.e. the limit of vanishing interfacial thickness. To study this limit we use the following scaling in the free energy

$$E^\gamma(c,u) := \int_\Omega \left(\tfrac{\gamma}{2}|\nabla c|^2 + \tfrac{1}{\gamma}\psi(c) + W(c,\mathcal{E}(u)) \right).$$

In this scaling the interfacial layer is of a thickness proportional to γ. For simplicity we assume in this section that ψ is of the form (2) with $a = 1$ and W is of the form (4). Our first goal is to derive the limit of E^γ as γ tends to zero. It turns out that the notion of Γ-limes is appropriate in order to pass to the limit $\gamma \to 0$. We will study solutions of the variational problem

($\mathbf{P}^\gamma$). Find a minimizer $(c,u) \in H^1(\Omega) \times X_{\text{ird}}^\perp$ of E^γ subject to the constraint $\fint_\Omega c = m$ where $m \in (-1,1)$ is a given constant.

We will see that solutions of ($\mathbf{P}^\gamma$) converge along subsequences to minimizers of the functional

$$E^0 : L^1(\Omega) \times X_{\text{ird}}^\perp \to \mathbb{R} \cup \{\infty\}$$

with

$$E^0(c,u) = \begin{cases} \sigma \mathcal{H}^{n-1}(\partial\{c=1\} \cap \Omega) + \int_\Omega W(c,\mathcal{E}(u)) \\ \qquad \text{if} \quad c \in BV(\Omega;\{-1,1\}) \quad \text{and} \quad \fint_\Omega c = m, \\ \infty \qquad \text{otherwise.} \end{cases}$$

Here $\sigma = \int_{-\infty}^{\infty} (\frac{1}{2}(z'(y))^2 + \psi(z(y)))dy$ where z is a solution of

$$-z'' + \psi'(z) = 0 \quad \text{with} \quad z(-\infty) = -1 \quad \text{and} \quad z(\infty) = 1.$$

One easily computes that

$$\sigma = \int_{-1}^{1} \sqrt{2\psi(s)}ds.$$

Theorem 4.1 *Let the assumptions stated above hold. Then it holds:*

i) For all $(c^{\gamma_\kappa}, u^{\gamma_\kappa})_{\kappa\in\mathbb{N}} \in H^1(\Omega) \times X_{ird}^{\perp}$ *with* $c^{\gamma_\kappa} \to c$ *in* $L^1(\Omega)$ *and* $u^{\gamma_\kappa} \to u$ *in* $L^2(\Omega, \mathbb{R}^d)$ *as* γ_κ *tends to zero, it holds*

$$E^0(c,u) \leq \liminf_{\kappa\to\infty} E^{\gamma_\kappa}(c^{\gamma_\kappa}, u^{\gamma_\kappa}).$$

ii) For any $(c,u) \in L^1(\Omega) \cap X_{ird}^{\perp}$ *and any sequence* $\gamma_\kappa \searrow 0$, $\kappa \in \mathbb{N}$, *there exists a sequence* $(c^{\gamma_\kappa}, u^{\gamma_\kappa})_{\kappa\in\mathbb{N}} \in H^1(\Omega) \cap X_{ird}^{\perp}$ *with* $c^{\gamma_\kappa} \to c$ *in* $L^1(\Omega)$ *and* $u^{\gamma_\kappa} \to u$ *in* $L^2(\Omega, \mathbb{R}^d)$ *as* $\gamma_\kappa \searrow 0$ *such that*

$$E^0(c,u) \geq \limsup_{\kappa\to\infty} E^{\gamma_\kappa}(c^{\gamma_\kappa}, u^{\gamma_\kappa}).$$

iii) Let (c^γ, u^γ) *be solutions of problem* $(\mathbf{P}^\gamma)$. *Then there exists a sequence* $\gamma_\kappa \to 0$, $\kappa \in \mathbb{N}$, *and a* $(c,u) \in L^2(\Omega) \times X_{ird}^{\perp}$ *such that*

$$\begin{aligned} c^{\gamma_\kappa} &\to c \quad \text{in} \quad L^2(\Omega), \\ u^{\gamma_\kappa} &\to u \quad \text{in} \quad H^1(\Omega, \mathbb{R}^d) \end{aligned}$$

and (c,u) *is a global minimizer of* E^0.

Remarks: a) The results i) and ii) of the preceding theorem state that E^0 is the Γ-limit of E^γ.

b) Result iii) gives that minimizers of E^γ approximate minimizers of a functional for partitionings of Ω under a volume constraint. This functional contains a term taking interfacial energy – in fact just the perimeter of the interface – into account and a term measuring the energy resulting from elastic stresses.

c) Regularity theory for minimizers of E^0 is an area which is totally unexplored yet (see Lin [58] for related results).

4.2 The Sharp Interface Limit of the Cahn-Larché System

In the preceding subsection we studied the sharp interface limit purely on a variational basis, i.e. one studies the convergence of the free energy as the interfacial energy tends to zero. Another goal would be to pass to the limit in the Cahn-Larché system itself. On this only results based on formally matched asymptotic expansions (see [56]) and a result for stationary solutions which are energy minimizing are known (see [37]).

Let me first mention the asymptotic limit of the Cahn-Hilliard equation. It is well established that in the limit $\gamma \to 0$ the chemical potentials w^γ tend to a limit w and the c^γ

tend to function c which takes values ± 1. The set $\Gamma = \partial\{c = 1\} \cap (\Omega \times (0,\infty))$ is the free boundary which we write as

$$\Gamma = \bigcup_{t>0} \Gamma_t \times \{t\}.$$

The limit (w,Γ) solves the following free boundary problem (for simplicity we always assume that $\Gamma_t \subset\subset \Omega$)

(MS) Mullins-Sekerka problem:

$$\begin{aligned} \Delta w &= 0 && \text{in} && \Omega\setminus\Gamma_t && , \ t>0, \\ \nabla w \cdot n &= 0 && \text{on} && \partial\Omega && , \ t>0, \\ \sigma\kappa &= 2w && \text{on} && \Gamma_t && , \ t>0, \\ 2V &= -[\nabla w]\cdot \nu && \text{on} && \Gamma_t && , \ t>0 \end{aligned} \tag{19}$$

where V is the normal velocity of the interface (where the normal is pointing into the region $\{c=1\}$), κ is the sum of the principal curvatures of Γ_t (which we will call, as frequently used, different to its original meaning the mean curvature) and ν is the normal pointing into the set $\{c=1\}$. We take the sign convention that a ball with $c=-1$ inside and $c=1$ outside has negative curvature. By $[g]$ we always denote the jump of a quantity g across the interface. More precisely we set

$$[g](x) := \lim_{\substack{\delta\to 0 \\ \delta>0}} (g(x+\delta\nu) - g(x-\delta\nu)).$$

For the moment we consider the case $W=0$. Then an absolute minimizer c of E^0 solves (19) with a constant w. An absolute minimizer of E^0 has constant mean curvature and w is up to the constant $\frac{\sigma}{2}$ equal to this mean curvature (see Giusti [46]). If we now consider absolute minimizers c^γ of E^γ, a constant Lagrange multiplier stemming from the mean value constraint appears. We have

$$-\gamma\Delta c^\gamma + \tfrac{1}{\gamma}\psi'(c^\gamma) = w^\gamma$$

where w^γ is a constant. In fact (c^γ, w^γ) is a solution of the Cahn-Hilliard equation. It was shown by Luckhaus and Modica [60] that the Lagrange multipliers w^γ of a converging sequence $c^\gamma \to c$ in $L^2(\Omega)$ converge to a constant w which is up to the factor $\frac{\sigma}{2}$ the mean curvature of the hypersurface $\partial\{c=1\}$ (which of course is a minimizer of E^0).

Now we consider the case $W \neq 0$. If (c,u) is a minimizer of E^0 it can be shown that a constant Lagrange multiplier w exists such that (see [37])

$$\sigma\kappa + \nu\cdot[W\,\mathrm{Id} - (\nabla u)^T W_{,\mathcal{E}}]\nu = 2w. \tag{20}$$

The quantity $\nu\cdot[W\,\mathrm{Id} - (\nabla u)^T W_{,\mathcal{E}}]\nu$ modifies the law that minimizers are constant mean curvature surfaces. Equation (20) and the non-equilibrium analogue (25) can be interpreted as a generalized Gibbs-Thomson equation (see [33], [54], [17] and [57]).

If we consider absolute minimizers (c^γ, u^γ) of E^γ, we also obtain Lagrange multipliers w^γ which fulfill (in a distributional sense)

$$-\gamma\Delta c^\gamma + \tfrac{1}{\gamma}\psi'(c^\gamma) + W_{,c}(c^\gamma, \mathcal{E}(u^\gamma)) = w^\gamma.$$

It is now also possible to show that the Lagrange multipliers w^γ converge (along subsequences) to a Lagrange multiplier w of the sharp interface variational problem. More precisely we obtain (see Garcke [37]):

Theorem 4.2 *Let Ω be a domain with a C^1-boundary and let $(c^\gamma, u^\gamma) \in H^1(\Omega) \cap X_{ird}^\perp$ be a solution of the variational problem $(\mathbf{P}^\gamma)$ with Lagrange multipliers w^{γ_κ}. Then for each subsequence $(\gamma_\kappa)_{\kappa\in\mathbb{N}} \searrow 0$ such that*

$$\begin{aligned} c^{\gamma_\kappa} &\to c \quad \text{in} \quad L^1(\Omega), \\ u^{\gamma_\kappa} &\to u \quad \text{in} \quad L^2(\Omega, \mathbb{R}^d) \end{aligned}$$

it holds

$$w^{\gamma_\kappa} \to w,$$

where w is the Lagrange multiplier for the absolute minimizer (c,u) of E^0 (see (20)).

Let us finally state the full moving boundary problem for the case with elastic effects. A triple (w,u,Γ) solves the generalized Mullins-Sekerka problem if the following conditions are fulfilled.

(GMS) Generalized Mullins-Sekerka problem:

$$\Delta w = 0 \quad \text{in} \quad \Omega\setminus\Gamma_t, \quad t>0, \tag{21}$$

$$\nabla \cdot W_{,\mathcal{E}}(c, \mathcal{E}(u)) = 0 \quad \text{in} \quad \Omega\setminus\Gamma_t, \quad t>0, \tag{22}$$

$$\nabla w \cdot n = 0 \quad \text{on} \quad \partial\Omega, \quad t>0, \tag{23}$$

$$(W_{,\mathcal{E}})n = 0 \quad \text{on} \quad \partial\Omega, \quad t>0, \tag{24}$$

$$\sigma\kappa + \nu \cdot [W\mathrm{Id} - (\nabla u)^T W_{,\mathcal{E}}]\nu = 2w \quad \text{on} \quad \Gamma_t, \quad t>0, \tag{25}$$

$$2V = -[\nabla w]\cdot\nu \quad \text{on} \quad \Gamma_t, \quad t>0, \tag{26}$$

$$[u] = 0 \quad \text{on} \quad \Gamma_t, \quad t>0, \tag{27}$$

$$[W_{,\mathcal{E}}\nu] = 0 \quad \text{on} \quad \Gamma_t, \quad t>0. \tag{28}$$

This sharp interface problem was derived in [56] from (5)-(7) with the help of formal asymptotic expansions. We remark that the set of equations can be simplified if we formulate them in a distributional sense. Then we would ask for functions $u : [0,T] \to H^1(\Omega)$, $c : [0,T] \to BV(\Omega, \{-1,1\})$ and $w : [0,T] \to H^1(\Omega)$ such that (25) is fulfilled together with the following equations

$$\partial_t c = \Delta w \quad \text{in } \Omega\times(0,T), \tag{29}$$

$$\nabla \cdot W_{,\mathcal{E}} = 0 \quad \text{in } \Omega\times(0,T). \tag{30}$$

All these equations have to hold in a weak sense. For example (26) is the jump condition obtained from (29) which has to hold since c jumps across the interface Γ (see [37] for details). The jump condition (27) results from the fact that $u(t) \in H^1(\Omega)$ and (28) is the jump condition resulting from (30). In the habilitation thesis [37] also a weak formulation

of (25) is formulated which generalizes a weak formulation of Luckhaus [59] to the case with mechanical effects. This formulation has the feature that mechanical effects enter into the weak formulation only through bulk terms which makes the analysis of the elasticity term much easier.

Remark 4.1 *i) It can be computed that the energy E^0 decreases in time for a solution of (21)-(28). In fact we have*

$$\frac{d}{dt}\left[\sigma\mathcal{H}^{n-1}(\partial\{c=1\}\cap\Omega)+\int_\Omega W(c,\mathcal{E}(u))\right]+\int_\Omega|\nabla w|^2=0.$$

ii) Existence of solutions to (21)-(28) is still an open problem. For related results in the situation without elasticity we refer to [22], [61], [12], [43] and [73]. A rigorous asymptotic analysis for $\gamma\searrow 0$ in the case without elastic effects has been given by [1], [21] and [76].

5 Surface Diffusion and Elastic Interactions

5.1 Surface Diffusion in the Presence of Stress and Electromigration

The Cahn-Hilliard equation can be interpreted as a phase field model, i.e. a model in which an interface between different phases is described with the help of a new continuum field (the phase field) which varies smoothly across the interface and which attains fixed but different values in the pure phases. The phase field approach has been applied successfully in a number of application areas. In particular it has been successfully used to model the solidification of pure substances. We refer to Chen [19] and Boettinger, Warren, Beckermann and Karma [9] for recent reviews on the phase field approach. The main goal of this section is to demonstrate that a Cahn-Larché system with a degenerate mobility can be used to model surface diffusion in the presence of elastic stresses. In this context the Cahn-Larché system is just a phase field model with c as the phase field which takes the values ± 1 in the two physically different states. In the applications we have in mind, $c=1$ will correspond to solid and $c=-1$ will correspond to vapour.

We would like to model situations in which the free surface of a solid changes its shape due to the diffusion of atoms along the surface. If this process is driven by capillarity, Mullins [70] (see also [23]) proposed the surface diffusion flow

$$V=-\nabla_s\cdot D_s\nabla_s(\sigma\kappa) \tag{31}$$

where V is the normal velocity of the evolving free surface, $\nabla_s\cdot$ is the surface divergence, D_s is a constant related to the surface diffusivity, ∇_s is the surface gradient, σ is the surface tension and κ is the mean curvature. If an interface is governed by the evolution law (31), atoms will move along the surface from regions with small curvature to regions with a higher curvature (see Figure 6). This law governs the evolution of interfaces in many applications, but often additional effects have to be accounted for (see below).

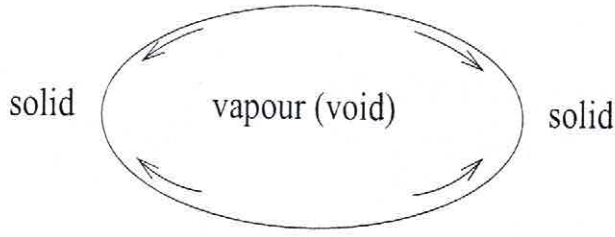

Figure 6: Surface diffusion from regions with small curvature to regions with higher curvature

It was shown by Cahn, Elliott and Novick-Cohen [14] with the help of formally matched asymptotic expansions that the surface diffusion flow is the asymptotic limit of the following degenerate Cahn-Hilliard equation

$$\begin{aligned} \gamma \partial_t c &= \nabla \cdot (\tfrac{8}{\pi} D_s b(c) \nabla w), \\ w &= \sigma \tfrac{2}{\pi} (-\gamma \Delta c + \tfrac{1}{\gamma} \psi'(c)). \end{aligned}$$

Here $b(c) = \max(0, 1 - c^2)$ and ψ is given by the double obstacle form (3) (where we take $R\theta_c = 1$ for simplicity). For the mathematical analysis of the degenerate Cahn-Hilliard equation we refer to [29] and for existence and stability results for the surface diffusion flow we refer to [30] and [34]. We only remark that the degeneracy of b for $c \notin (-1, 1)$ leads to severe difficulties in the analysis of this fourth order degenerate parabolic equation.

The motion of voids in interconnects in integrated circuits and the evolution of the surface of a thin film in heteroepitaxial growth is driven by surface diffusion, but now additional effects have to have accounted for. In the latter case elastic stresses arise due to the elastic mismatch between the film and the substrate. These lead to an instability of an initially planar film (see [2], [47] and also [36] for a recent review). For void motion elastic stresses are important, but also transport phenomena due to a drift resulting from an electric field will play a role (electromigration).

Recently phase field models based on the Cahn-Hilliard theory have been proposed to model these phenomena [62, 7, 26, 3, 4, 5]. Let us briefly discuss how these phenomena modify the surface diffusion law (31). If we denote by $W_1(\mathcal{E})$ the elastic energy density of the solid and by ϕ the electric potential, we obtain

$$V = \nabla_s \cdot D_s \nabla_s (-\sigma \kappa + W_1(\mathcal{E}(u)) + \alpha \phi).$$

The second term on the right hand side leads to a flux of atoms from regions on the surface with high elastic energy to regions on the surface with less elastic energy (see Figure 7). If the constant α is negative the third term leads to diffusion in the direction opposite to the electric field (see Figure 8). The phase field model studied in the papers [3, 4] is now given

by

$$\gamma \partial_t c = \nabla \cdot (\tfrac{8}{\pi} D_s b(c)) \nabla w, \tag{32}$$

$$w = \sigma \tfrac{2}{\pi} (-\gamma \Delta c + \tfrac{1}{\gamma} \psi(c)) + \tfrac{1}{2} d'(c) \mathcal{E}(u) : \mathcal{E}(u) + \alpha \phi \tag{33}$$

where

$$d(s) := c_0 + \tfrac{1}{2}(1 - c_0)(1 + s)$$

is an interpolation function with $c_0 = c_0(\gamma) \to 0$ as $\gamma \to 0$. These equations are coupled to a quasi-static equilibrium for u, i.e.

$$\nabla \cdot S = 0 \,, \; S = W_{,\mathcal{E}}(c, \mathcal{E}(u)) = d(c) C \mathcal{E}(u)$$

where

$$W(c, \mathcal{E}(u)) = \tfrac{1}{2} d(c) C \mathcal{E}(u) : \mathcal{E}(u).$$

The above equations are coupled to boundary conditions which we take to be (although other boundary conditions are possible)

$$\nabla c \cdot n = 0, \nabla w \cdot n = 0, Sn = \overline{S} n$$

where $\overline{S}$ is a given tensor describing outer applied stresses. For variants of this model (which have been proposed earlier) we refer to [62, 7, 26].

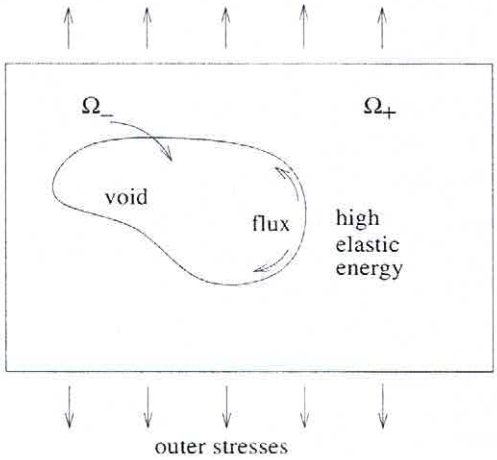

Figure 7: Surface diffusion driven by elastic energy. Atoms diffuse away from regions with high elastic energy.

There are two a priori estimates for the above system which are crucial. One is the decay of the free energy which reads as follows (for $\alpha = 0$)

$$\frac{d}{dt} \int_\Omega \left[\sigma \tfrac{2}{\pi} \left\{ \tfrac{\gamma}{2} |\nabla c|^2 + \tfrac{1}{\gamma} \psi(c) \right\} + W(c, \mathcal{E}(u)) - \mathcal{E}(u) : \overline{S} \right] + \tfrac{1}{\gamma} \int_\Gamma b(c) |\nabla w|^2 \leq 0.$$

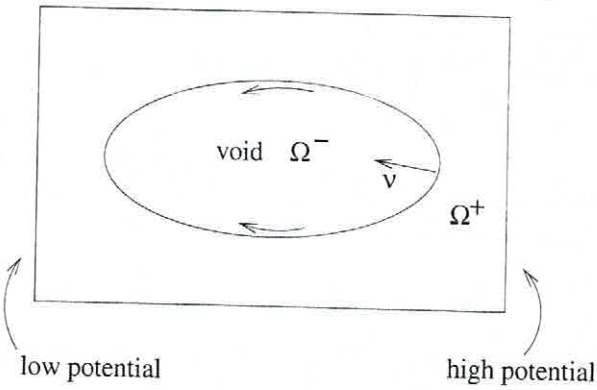

Figure 8: Surface diffusion driven by an electric field. Here an example where the diffusion is against the electric field.

This a priori estimate was the basic ingredient in the analysis for the Cahn-Larché system with constant mobility (see [37, 38, 39]). In the case that the mobility depends on the concentration and degenerates this estimate is not enough for a successful mathematical analysis. Already in the case without elasticity one needs a so called "entropy" estimate (basically another integral estimate) to obtain enough information to show existence of a solution. If we try to obtain such an estimate in the case with elasticity, we obtain (for simplicity we take $D_s = \frac{\pi}{8}$ and $\sigma = \frac{\pi}{2}$)

$$\gamma^2 \frac{d}{dt} \int_\Omega G(c) + \tfrac{1}{2}\gamma^2 \int_\Omega |\Delta c|^2 \leq \int_\Omega |\nabla c|^2 + \tfrac{1}{32} \mathcal{M}_c \int_\Omega |\mathcal{E}(u)|_2^4 \tag{34}$$

where G is a function such that

$$G''(s) = \frac{1}{b(s)}.$$

The above estimate follows relatively straight forward using the properties of W, ψ, b and G, integration by parts and Young's inequality. The main problem is now to control the right hand side of (34). The term $\int_\Omega |\nabla c|^2 dx$ is controlled via the energy inequality. The difficult part is to control the last term which is quartic in $\mathcal{E}(u)$.

Let us demonstrate formally how this can be done in two space dimensions. The first attempt would be to use the Gagliardo-Nirenberg inequality which for $d = 2$ gives

$$\|\nabla u\|_{L^4} \leq C \left(\|u\|_{H^{2,2}}^{\frac{1}{2}} \|\nabla u\|_{L^2}^{\frac{1}{2}} + 1 \right). \tag{35}$$

Then we can use regularity theory for the displacement u. In fact u solves the system

$$\nabla \cdot (C\mathcal{E}(u)) = \tfrac{-1}{d(c)} C\mathcal{E}(u) \nabla d(c)$$

and hence if a $H^{2,2}$-regularity theory is known for the system $\nabla \cdot (C\mathcal{E}(u)) = r.h.s.$ one obtains from (35) (using again a Gagliardo-Nirenberg inequality) that

$$\|\nabla u\|_{L^4}^4 \leq \tilde{C}(1 + \|\Delta c\|_{L^2}^2).$$

This is not enough to control the right hand side in (34). In fact the growth is just critical. To obtain sufficient estimates it is necessary to first show that

$$\exists\, \varepsilon > 0 \text{ such that } \nabla u \in L^{2+\varepsilon}(\Omega).$$

This can be done e.g. with methods as in [39]. Then a sharper variant of the Gagliardo-Nirenberg inequality yields that there exists a $\delta > 0$ such that

$$\int_\Omega |\nabla u|^4 \leq \tilde{c} \left((\int_\Omega |\Delta c|^2)^{2-\delta} + 1 \right).$$

Hence we have a subcritical growth of $\int_\Omega |\mathcal{E}(u)|_2^4$ on the right hand side in (34) and we can proceed.

These arguments are purely formal. For a rigorous existence result in two space dimensions which is obtained by showing convergence of a finite element method we refer to [3].

5.2 Numerical Simulations for Void Migration

Electro- and stressmigration along interfaces plays a crucial role in the failure of metallic interconnects in microelectronic devices. A theoretical understanding of these phenomena is therefore of great practical interest. In this subsection we will present some numerical simulations for void migration obtained by solving the model presented in Subsection 5.1 with the help of a finite element method (for details we refer to [3], [4] and [5]). All numerical simulations in this section are a result of a collaboration with John Barrett and Robert Nürnberg (Imperial College, London) and the computations were performed by Robert Nürnberg.

In Figure 9 a numerical experiment is shown for stressmigration alone, i.e. we solve (32), (33) with $\alpha = 0$. In the experiment shown in Figure 9 we started with two voids, isotropic elasticity and tensile forces to the right and to the left (for more details on the setup of the numerical experiments we refer to [3], [5]). At the bottom to the right the elastic energy is displayed and one clearly sees that material is transported away from regions with high elastic energy. We remind the reader that the material transport though is only along the interface. The mass diffusion finally leads to a cut in the interconnect (Figure 9).

In Figure 10 we start with one void and have tensile forces at the top and at the bottom. We illustrate by grey shades the strength of the elastic energy and it is clearly seen in this figure how mass transport due to a high elastic energy at some parts of the interface leads to a severe change in shape. We refer to [3], [5] for more drastic examples also showing a crack-like behaviour.

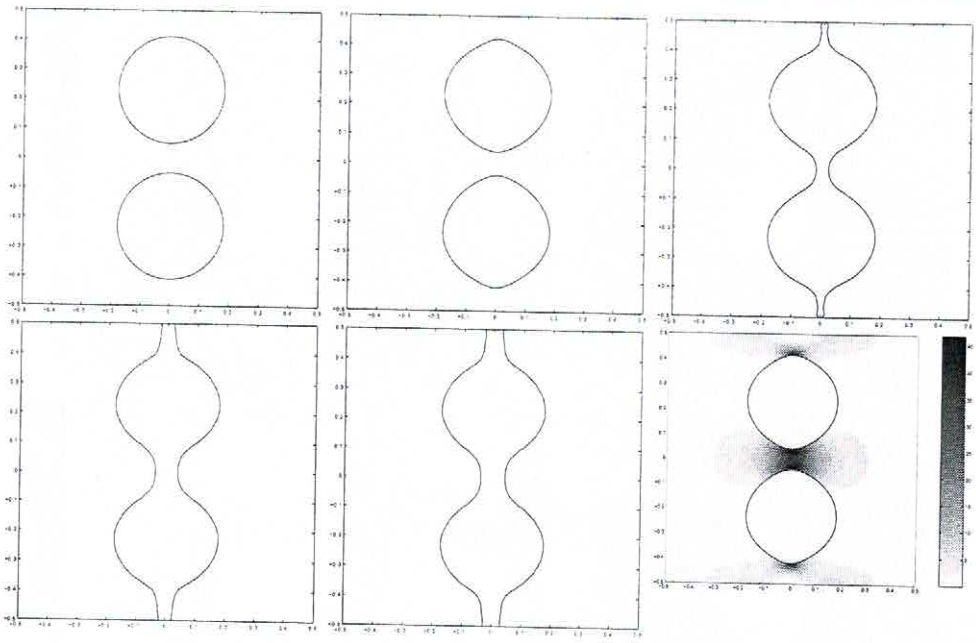

Figure 9: ($\overline{S} = \left(\begin{smallmatrix} 1 & 0 \\ 0 & 0 \end{smallmatrix}\right)$) Zero level sets for $c(x,t)$ at times $t = 0,\ 10^{-5},\ 2\times 10^{-5},\ 2.5\times 10^{-5},\ 5\times 10^{-5}$ and elastic energy at time t=10^{-5}.

In Figure 11 we show the combined effect of electro- and stressmigration. We start with a circular void on the right and the other shapes are the solution at different times. The electric field induces a mass transport from the right to the left leading to the migration of the void to the right. The elastic field leads to a deformation of the void (see [6] for computations with electro- but no stressmigration).

5.3 Heteroepitaxial Thin Film Growth

Also in heteroepitaxial growth of thin solid films, diffusion of atoms along an interface (surface diffusion) is driven in such a way that an energy which contains surface energy as well as elastic energy decreases. Here elastic stresses result from an elastic mismatch between the substrate and the film (see Figure 12). For a discussion of the sharp interface model we refer to Gao and Nix [36] and Spencer, Davis and Voorhees [75]. The normal velocity of the sharp interface is now given by

$$V = \nabla_s \cdot D_s \nabla_s (-\sigma\kappa + \tfrac{1}{2} C(\mathcal{E}(u) - \overline{\mathcal{E}}) : (\mathcal{E}(u) - \overline{\mathcal{E}}))$$

where $\overline{\mathcal{E}}$ is the mismatch strain between film and substrate, where we choose the unstressed substrate lattice as reference configuration. In this context we either specify Dirichlet boundary conditions for u at the film-substrate interface (rigid substrate) or we need to solve an elasticity system in the substrate as well.

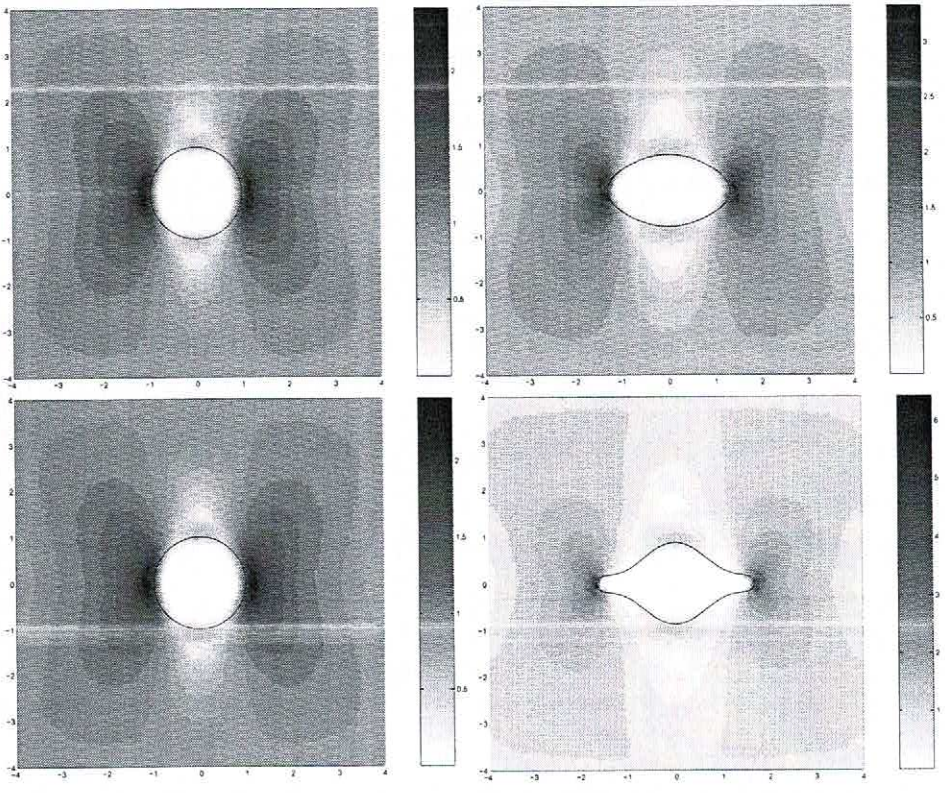

Figure 10: Elastic stress field for small elastic constants at times $t = 0,\ 2$ (above) and for larger elastic constants at times $t = 0,\ 0.1$ (below).

In the Cahn-Hilliard phase field model we now obtain

$$\gamma\partial_t c = \nabla \cdot (\tfrac{8}{\pi} D_s b(c)) \nabla \left[\sigma \tfrac{2}{\pi} (-\gamma \Delta c + \tfrac{1}{\gamma} \psi'(c)) + \tfrac{1}{2} d'(c) C(\mathcal{E}(u) - \overline{\mathcal{E}}) : (\mathcal{E}(\overline{u}) - \overline{\mathcal{E}}) \right].$$

This equation coupled to an elasticity system has been studied by Barrett, Garcke and Nürnberg [5]. A similar model has been studied earlier by Eggleston [25] and Eggleston and Voorhees [26].

In the Figures 13, 14 we show how an initially planar film becomes unstable due to the presence of elastic forces. There are actually parts of the film where the film height becomes zero. When this happens the energetics of the film —vapour— substrate triple point becomes important. In fact in experiments a wetting layer in front of a zero contact angle forms (see [74]) and the correct modelling of this issue together with simulation in three space dimension is work in progress.

We remark that there is the hope that the formation of islands (as seen in Figure 14) can be used to produce quantum-dot-based devices and it is the challenge to control the formation of islands such that a large number of spatially ordered islands ("quantum dots") form. Here theoretical modelling and numerical simulations will play an important role (see the conclusion section of [36]).

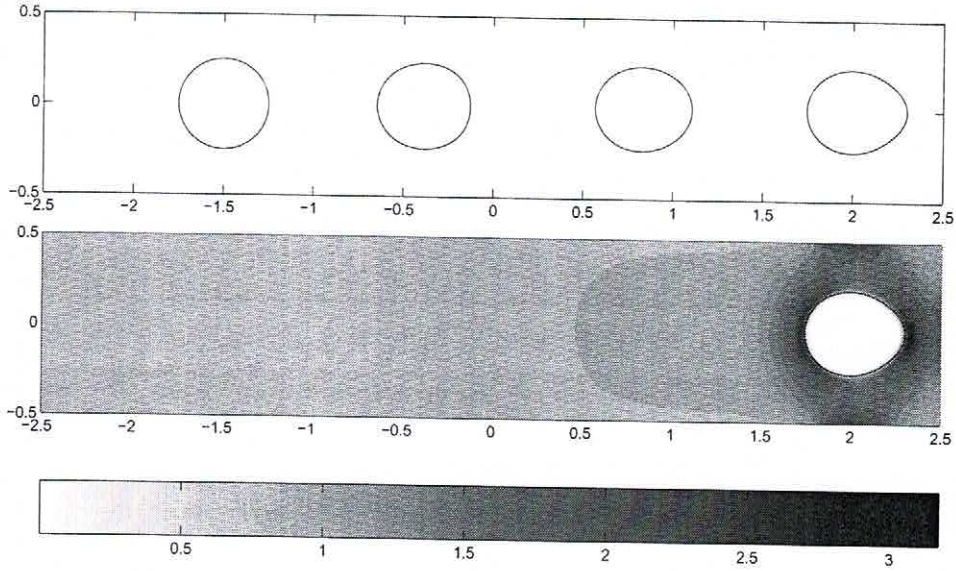

Figure 11: ($\alpha = 40\pi$, isotropic elasticity, $\overline{S} = \left(\begin{smallmatrix} 1 & 0 \\ 0 & 1 \end{smallmatrix}\right)$) Zero level sets for $c(x,t)$ at times $t = 0, 1.2 \times 10^{-3}, 2.5 \times 10^{-3}, T = 3.75 \times 10^{-3}$ (above) and the elastic energy at time $T = 3.75 \times 10^{-3}$.

6 Numerical Approximation

6.1 The Discrete Problem

When designing a numerical method to approximate a partial differential equation it is always a good idea to come up with a discrete problem which inherits as many properties as possible from the continuous problem. Since the continuous problem (5)-(7) has a variational structure, it is natural to use a finite element method. The equation for the concentration c is of fourth order. From an implementation point of view, it is desirable to use finite elements with an ansatz space which contains polynomials with low order. Therefore splitting methods are very popular to approximate fourth order parabolic equations (see e.g. [28]). In a splitting method for the Cahn-Hilliard equation finite element spaces of continuous piecewise affine elements are used to approximate the concentration c and the chemical potential w. We will also use this ansatz space for the displacement u.

We will assume in this section that Ω is a polyhedral domain. Then we choose a quasi-uniform family $\{\mathcal{T}^h\}_{h>0}$ of partitionings of Ω into disjoint simplices with maximal element size $h := \max_{s \in \mathcal{T}^h} \{\operatorname{diam} s\}$, so that $\overline{\Omega} = \bigcup_{s \in \mathcal{T}^h} \overline{s}$. Associated to $\mathcal{T}^h$ is the finite element space of continuous piecewise affine elements

$$S^h := \{\varphi \in C^0(\overline{\Omega}) \mid \varphi_{|S} \text{ is linear for all } S \in \mathcal{T}^h\} \subset H^1(\Omega).$$

To formulate a finite element discretization we introduce the lumped mass scalar

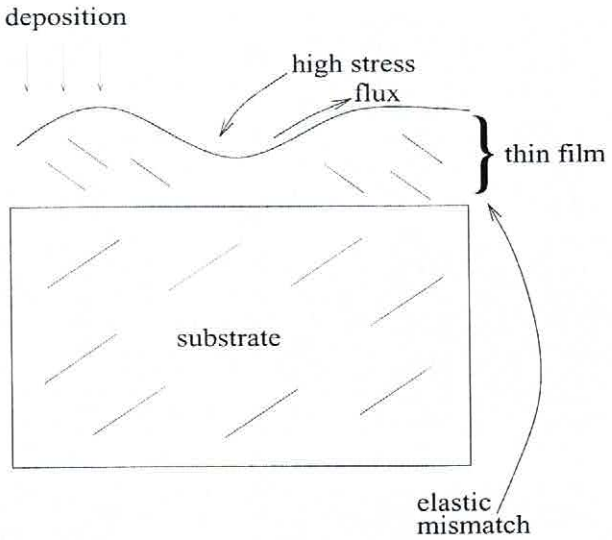

Figure 12: Surface diffusion in heteroepitaxial thin film growth.

product $(\cdot,\cdot)^h$ instead of the L^2 scalar product $(\cdot,\cdot)$ as follows: For $v_1, v_2 \in C^0(\overline{\Omega})$ let

$$(v_1, v_2)^h := \int_\Omega \pi^h(v_1 v_2)$$

where $\pi^h : C^0(\overline{\Omega}) \to S^h$ is the interpolation operator, such that $(\pi^h \eta)(p) = \eta(p)$ for all nodes of $\mathcal{T}^h$.

Then a semi-implicit scheme for (5)-(7) reads as follows (we set $b = 1$).

We search for $c^n, w^n : [0,T] \to S^h$ and $u^n : [0,T] \to (S^h)^d$ such that

$$\begin{aligned}
(\partial_t c^h, \varphi^h)^h &= -(\nabla w^h, \nabla \varphi^h), && (36)\\
(w^h, \varphi^h)^h &= \gamma(\nabla c^h, \nabla \varphi^h) + (\psi'(c^h), \varphi^h)^h + (W_{,c}(c^h, \mathcal{E}(u^h)), \varphi^h), && (37)\\
0 &= (\mathcal{E}(u^h) - \overline{\mathcal{E}}(c^h), C(\rho^h)\mathcal{E}(\xi^h)) && (38)
\end{aligned}$$

holds for all $\varphi^h \in S^h, \xi^h \in (S^h)^d$ and all $t \in [0,T]$.

In order to obtain a fully discrete scheme one needs to introduce a time discretization. The simplest implicit time discretization is the implicit Euler scheme in which the time derivative in (36) is discretized in the following way

$$(\partial_t c^h, \varphi^h)^h \rightsquigarrow \left(\frac{c_n^h - c_{n-1}^h}{\tau_n}, \varphi^h \right)^h.$$

Here we devided the time intervall $[0,T]$ into N steps with length τ_n and set $t_n := \sum_{i=1}^n \tau_i$. The discrete solution at time t_n is denoted by (c_n^h, w_n^h, u_n^h). The resulting numerical scheme has been analyzed in [42, 44]. In [42] optimal error estimates have been shown in the

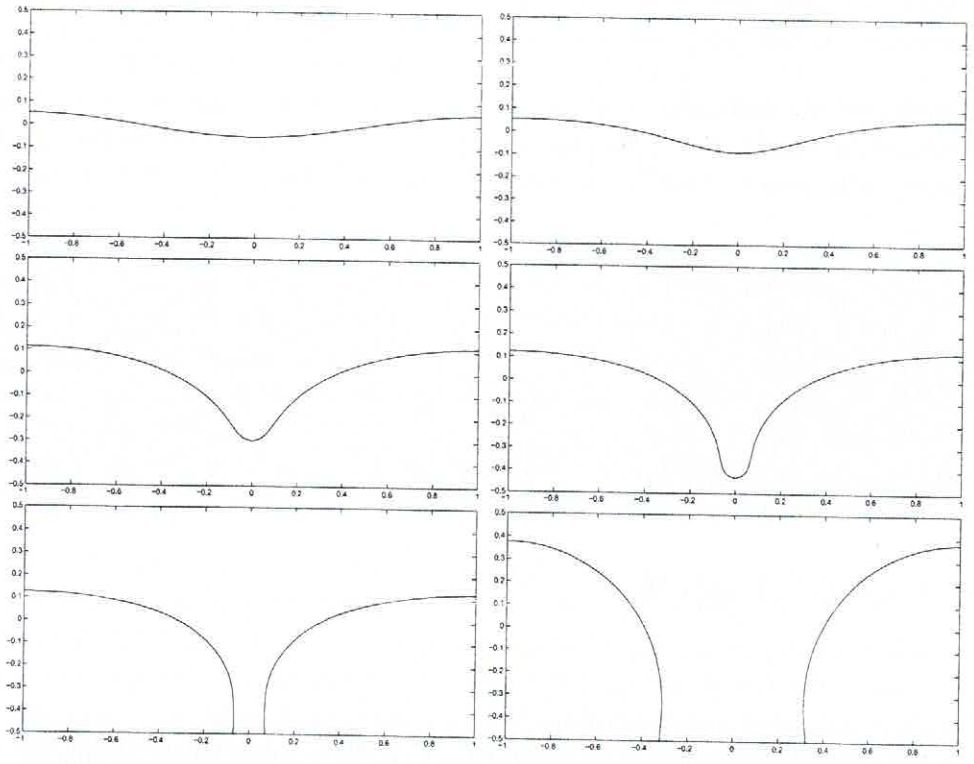

Figure 13: Instability of a nearly flat initial film. Appearance of regions with zero film height.

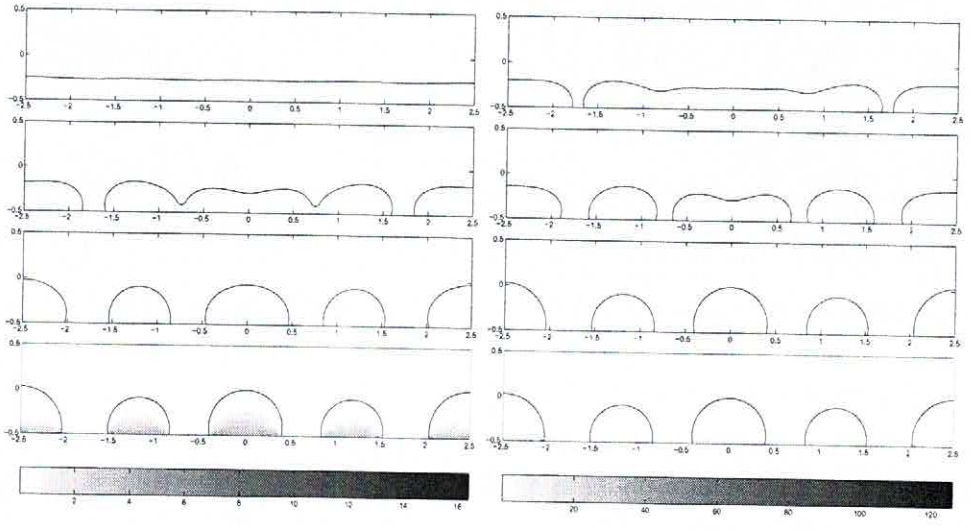

Figure 14: Island formation in thin film epitaxial growth.

case that C does not depend on the concentration (homogeneous elasticity). In the case of inhomogeneous elasticity a convergence proof has been given in [44].

Remark 6.1 *i) The fully discrete scheme has the properties that mass is conserved and that the total discrete free energy decreases (see [42, 44]). The last property is the discrete counterpart of inequality (8) and is an important property in the analysis of the scheme (see [44]).*
ii) It turns out that the so-called θ-scheme [11, 69] leads to a more efficient but hard to analyze time discretization. All the computations presented in the following are with the help of the θ-scheme, but we made sure that computations with the implicit Euler scheme lead to the same results although with more computational effort. The discrete linear systems were solved with the help of the BICG and GMRES algorithms and for the nonlinear discrete problem we used Newton's method.
iii) For the degenerate Cahn-Larché system a more sophisticated discretization has to be used and we refer to [3, 4, 5] for details.

6.2 Numerical Computations

In this subsection we present numerical simulations for the system (5)-(7) which were carried out with the method described in Subsection 6.1. All numerical simulations were part of the PhD thesis of Ulrich Weikard [77] (we also refer to [42] and [44]). For other approaches to solve the system (5)-(7) numerically which use spectral methods, we refer to Chen and Shen [20], Dreyer and Müller [24] and Leo, Lowengrub and Jou [56].

6.3 Anisotropic Homogeneous Elasticity

The first experiment (see Figure 15) shows the effect of anisotropic elasticity. The anisotropy was chosen to have cubic symmetry with a mismatch strain which was proportional to the identity. One clearly observes that the interfaces align along the coordinate axes.

In Figures 4 and 5 we already showed numerical computations for spinodal decomposition. The figures show the patterns arising without elasticity (see Figure 4) and with cubic anisotropy (see Figure 5). These patterns form at the beginning of the phase separation process. In both figures also the dominate Fourier modes are given and these are in agreement with the theory presented in Section 2. We remark that with isotropic elasticity one would obtain the same patterns as in Figure 4. For more details we refer to [40].

6.3.1 Effects of Inhomogeneous Elasticity

If the elastic constants differ (inhomogeneous elasticity), new phenomena occur. In Figure 16 we see that particles align and repell each other. The example shown is for a situation with cubic symmetry and with different elastic constants for the two components.

For the Cahn-Hilliard equation without mechanical effects one observes that only the phase with a smaller volume fraction can form the particles. If mechanical effects are

included in an inhomogeneous way, this is not always the case. In Figure 17 to the left we see a situation in which the phase with a larger volume fraction (the green phase) forms the particles on the long run although after spinodal decomposition the other phase formed the particles. If we interchange the elastic constants between the two components but keep the volume fraction, we see that the phase with the smaller volume fraction forms the particles. For more details on the numerical approximation of the Cahn-Larché system we refer to [42], [44] and to [56].

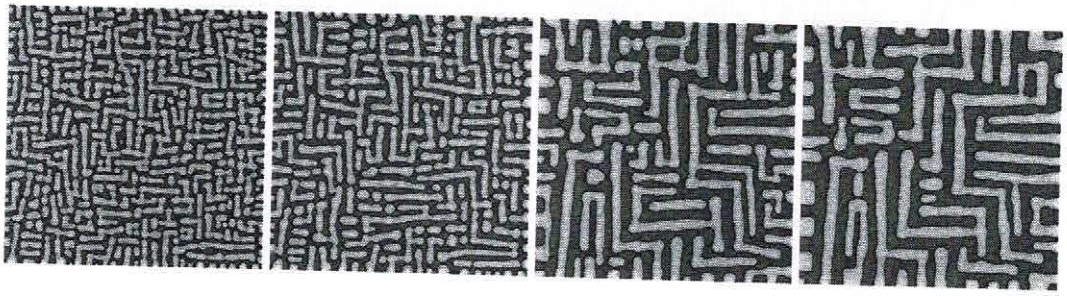

Figure 15: Patterns arising with homogeneous, cubic anisotropy. In contrast to the Figures 4 and 5 these patterns arise at large times.

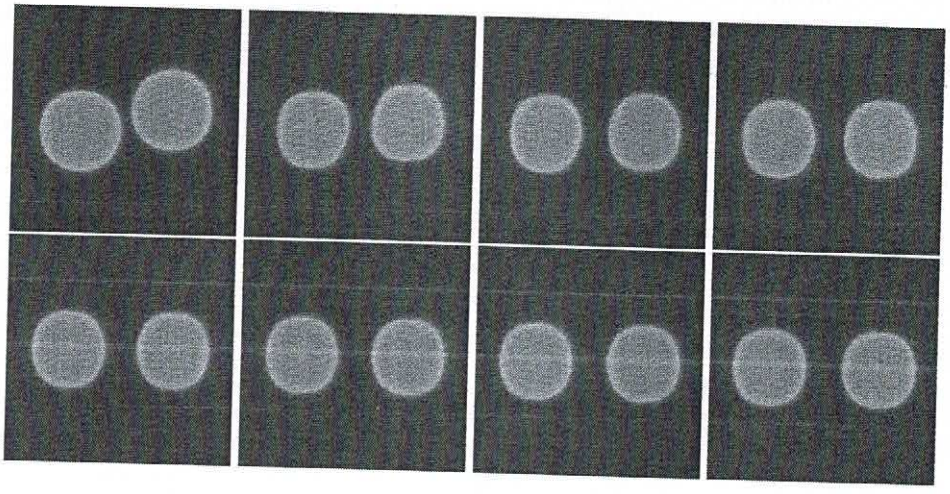

Figure 16: Alignment and repulsion of particles for inhomogeneous elasticity with cubic anisotropy.

Acknowledgments

The author would like to thank his coworkers John Barrett, Stanislaus Maier-Paape, Barbara Niethammer, Robert Nürnberg, Martin Rumpf and Ulrich Weikard for many discussions

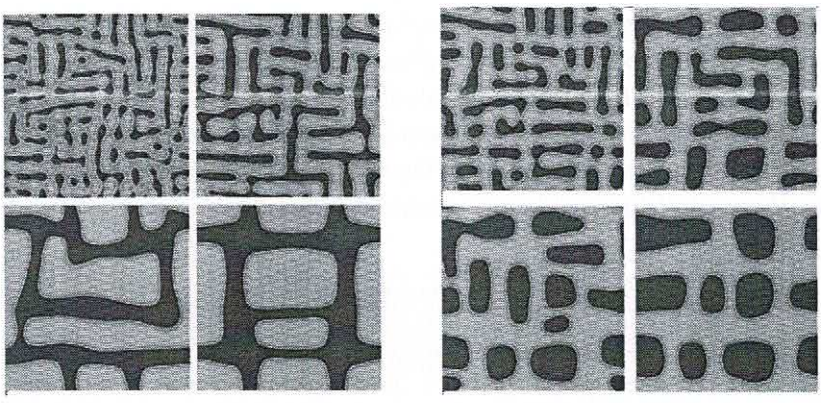

Figure 17: Two simulations that show that in the case of inhomogeneous elasticity also the phase with the larger volume fraction can form the particles (see the left simulation). In the simulation to the right we interchanged the elastic constants of the two components.

which helped me to understand many aspects of the Cahn-Larché system. I would also like to thank David Kwak who read and corrected first versions of this paper and Eva Rütz for typesetting my notes. The Figures 1-3 have been prepared by Stanislaus Maier-Paape, the Figures 4, 5, 15-17 are numerical simulations by Ulrich Weikard, the Figures 6-8 and 12 are due to Eva Rütz and the Figures 9-11, 13, 14 are numerical simulations by Robert Nürnberg. My thank goes to all of them.

I would like to thank Hans Wilhelm Alt and Charlie Elliott for introducing me to the mathematical theory of phase changes and to the Cahn-Hilliard theory. This work was supported by the DFG Priority Program "Analysis, Modeling and Simulation of Multiscale Problems".

References

[1] N. Alikakos, P. Bates, and X. Chen X., Convergence of the Cahn-Hilliard equation to the Hele–Shaw model, *Arch. Rat. Mech. Anal.* **128** (1994), pp. 165–205.

[2] R. J. Asaro and W.A. Tiller, Interface morphology development during stress corrosion cracking: Part i. via surface diffusion, *Met. Trans.* **3** (1972), pp. 1789–1793.

[3] J. W. Barrett, H.Garcke, and R. Nürnberg, Finite Element Approximation of a Phase Field Model for Surface Diffusion of Voids in a Stressed Solid, submitted (2004).

[4] J. W. Barrett, H.Garcke, and R. Nürnberg, A phase field model for electromigration of intergranular voids, in preparation (2004).

[5] J. W. Barrett, H.Garcke, and R. Nürnberg, Phase field models for stress and electromigration induced surface diffusion with applications to epitaxial growth and void evolution, in preparation (2004).

[6] J. W. Barrett, R. Nürnberg, and V. Styles, Finite element approximation of a void electromigration model, *SIAM J. Numer. Anal.* (2004) (to appear).

[7] D. N. Bhate, A. Kumar, and A.F. Bower, Diffuse interface model for electromigration and stress voiding, *J. Appl. Phys.* **87** (2000), pp. 1712–1721.

[8] J. F.Blowey and C. M.Elliott, The Cahn-Hilliard gradient theory for phase separation with nonsmooth free energy. I., Mathematical analysis. *European J. Appl. Math.* **2** (1991), no. 3, pp. 233–280.

[9] W. J. Boettinger, J. A. Warren, C. Beckermann and A. Karma, Phase-Field Simulations of Solidification, *Ann. Rev. Mat. Res.* **32** (2002), 163.

[10] E. Bonetti, P. Colli, W. Dreyer, G. Gilardi, G. Schimperna, and J. Sprekels, On a model for phase separation in binary alloys driven by mechanical effects, *Physica D* **165** (2002), pp. 48–65.

[11] M. O. Bristeau, R. Glowinski, and J. Periaux, Numerical methods for the Navier-Stokes equations: Applications to the simulation of compessible and incompressible viscous flows, In: Computer Physics Report, Research Report UH/MD-4. University of Houston, 1987.

[12] L. Bronsard, H. Garcke, and B. Stoth, A multi-phase Mullins-Sekerka system: matched asymptotic expansions and an implicit time discretisation for the geometric evolution problem, *Proc. Roy. Soc. Edinburgh*, **128** A(1998), pp. 481–506.

[13] J. W. Cahn, On spinodal decomposition, *Acta Metall.*, **9** (1961), pp. 795–801.

[14] J. W. Cahn, J. W., C. M. Elliott, and A. Novick-Cohen, The Cahn-Hilliard equation with a concentration dependent mobility: motion by minus the Laplacian of the mean curvature, *European J. Appl. Math.* **7** (1996), no. 3, 287–301.

[15] J. W. Cahn and J. E. Hilliard, Free energy of a nonuniform system. I. Interfacial free energy, *Journal of Chemical Physics*, Vol. 28 (1958), pp. 258–267.

[16] J. W. Cahn and F. C. Larché, A linear theory of thermomechanical equilibrium of solids under stress, *Acta Metall.*, **21** (1973), pp. 1051–1063.

[17] J. W. Cahn and F. C. Larché, Surface stress and the chemical equilibrium of single crystals. II. Solid particles imbedded in a solid matrix, *Acta Metal.* **30** (1982), 51–56.

[18] M. Carrive, A. Miranville, and A. Piétrus, The Cahn-Hilliard equation for deformable elastic media, *Adv. Math. Sci. App.* **10** (2000), pp. 539–569.

[19] L.-Q. Chen, Phase-field models for microstructure evolution, *Annu. Rev. Mater. Res.* **32** (2002), pp. 113-140.

[20] L.-Q. Chen and J. Shen, Application of Semi-Implicit Fourier-Spectral Method to Phase-Field Equations, *Computer Physics Communications* **108** (1998), pp. 147–158.

[21] X. Chen, Global asymptotic limit of solutions of the Cahn-Hilliard equation, *J. Differential Geom.* **44** (1996), no. 2, pp. 262–311.

[22] X. Chen, J. Hong, and F. Yi, Existence, uniqueness, and regularity of classical solutions of the Mullins-Sekerka problem, *Comm. Partial Differential Equations* **21** (1996), no. 11-12, pp. 1705–1727.

[23] F. Davi and M. E. Gurtin, On the motion of a phase interface by surface diffusion, *J. Appl. Math. and Phys.* **41** (1990), pp. 782–811.

[24] W. Dreyer and W. H. Müller, A study of the coarsening in tin/lead solders, *Int. J. Solids Struct.* **37** (2000), pp. 3481–3871.

[25] J. J. Eggleston, Phase-Field Models for Thin Film Growth and Ostwald Ripening, PhD thesis, Northwestern University, Evanston (2001).

[26] J. J. Eggleston and P. W. Voorhees, Ordered growth of nancrystals via a morphological instability, *Appl. Phys. L.* Vol. 80, No. 2 (2002), 306–308.

[27] C. M.Elliott, The Cahn-Hilliard model for the kinetics of phase transitions, in Mathematical Models for Phase Change Problems, J.F. Rodrigues (ed.), *International Series of Numerical Mathematics*, Vol. 88, Birkhäuser-Verlag, Basel, pp. 35–73.

[28] C. M. Elliott, D. A. French, and F. A. Milner, A 2nd order splitting method for the Cahn-Hilliard equation, *Num. Math.*, **54** (1989), pp. 575–590.

[29] C. M. Elliott and H. Garcke, On the Cahn-Hilliard equation with degenerate mobility, *SIAM J. Math. Anal.*, **27** (1996), pp. 404–423.

[30] C. M. Elliott and H. Garcke, Existence results for diffusive surface motion laws, *Adv. Math. Sci. Appl.* **7** (1997), pp. 465–488.

[31] C.M.Elliott and S. Luckhaus, A generalised diffusion equation for phase separation of a multi-component mixture with interfacial free energy, SFB256 University Bonn, Preprint 195 (1991).

[32] J. D. Eshelby, Elastic inclusions and inhomogeneities, *Prog. Solid Mech.*, **2** (1961), pp. 89–140.

[33] J. D. Eshelby, The elastic energy-momentum tensor, *J. Elasticity* **5** (1975), 321–336.

[34] J. Escher, U. F. Mayer, and G. Simonett, The surface diffusion flow for immersed hypersurfaces, *SIAM J. Math. Anal.*, **29**(1998), no.6, pp.1419-1433.

[35] P. Fratzl, O. Penrose, and J. L. Lebowitz, Modelling of phase separation in alloys with coherent elastic misfit, *J. Stat. Physics*, **95** 5/6 (1999), pp. 1429–1503.

[36] H. Gao and W. D. Nix, Surface Roughening of Heteroepitaxial Thin Films, *Annu. Rev. Mater. Sci* **29** (1999), pp. 173-209.

[37] H. Garcke, On mathematical models for phase separation in elastically stressed solids, habilitation thesis, University Bonn, (2000).

[38] H. Garcke, On Cahn-Hilliard systems with elasticity, *Proc. Roy. Soc. Edinburgh* , **133** A, (2003), pp. 307–331.

[39] H. Garcke, On a Cahn-Hilliard model for phase separation with elastic misfit, submitted (2004).

[40] H. Garcke, S. Maier-Paape, and U. Weikard, Spinodal decomposition in the presence of elastic interactions , A reprint from: S.Hildebrand/H.Karcher (Eds.), *Geometric Analysis and Nonlinear Partial Differential Equations*, Springer Verlag (2003).

[41] H. Garcke, B. Niethammer, M. Rumpf, and U. Weikard, Transient coarsening behaviour in the Cahn-Hilliard model, *Acta Mat.* **51** (2003), pp. 1823–2830.

[42] H. Garcke, M. Rumpf, and U. Weikard, The Cahn-Hilliard equation with elasticity: Finite element approximation and qualitative studies, *Interfaces and Free Boundaries*, **3** (2001), pp. 101–118.

[43] H. Garcke and T. Sturzenhecker, The degenerate multiphase Stefan problem with Gibbs-Thomson law, *Adv. Math. Sci. Appl.*, **8** (1998), pp. 929–941.

[44] H. Garcke and U. Weikard, Numerical approximation of the Cahn-Larché equation, submitted (2004).

[45] M. Giaquinta and G. Modica, Regularity results for some classes of higher order nonlinear elliptic systems, *J. für reine u. angew. Math.*, 311/312 (1979), pp. 145–169.

[46] E. Giusti, Minimal Surfaces and Functions of Bounded Variation, Birkhäuser Verlag, Basel, Boston, Stuttgart (1984).

[47] M. A. Grinfeld, Instability of the separation boundary between a non-hydrostatically stressed elastic body and a melt, *Soviet Physics Doklady* **31** (1986), pp. 831–834.

[48] M. E. Gurtin, The Linear Theory of Elasticity, *Handbuch der Physik*, Vol. VIa/2, Springer, S. Flügge and C. Truesdell (eds.), Berlin, 1972.

[49] M. E. Gurtin, An Introduction to Continuum Mechanics, *Academic Press*, New York, 1982.

[50] M. E. Gurtin, Generalised Ginzburg–Landau and Cahn–Hilliard equations based on a microforce balance, *Physica D*, **92** (1996), pp. 178–192.

[51] M. E. Gurtin and P. W. Voorhees, The continuum mechanics of coherent two-phase elastic solids with mass transport, *Proc. Royal Soc. London A*, **440** (1993), pp. 323–343.

[52] A. G. Khachaturyan, Theory of Structural Transformations in Solids, Wiley, New York (1983).

[53] T. Küpper, N. Masbaum, Simulation of paraticle growth and Ostwald ripening via the Cahn-Hilliard equation, *Acta Metall. Mater.* **42** (6) (1994), pp. 1847–1858.

[54] F. C. Larché and J. W. Cahn, Thermochemical equilibrium of multiphase solids under stress, *Acta Metall.* **26** (1978), pp. 1579–1589.

[55] F. C. Larché and J. W. Cahn, The effect of self–stress on diffusion in solids, *Acta Metall.*, **30** (1982), pp. 1835–1845.

[56] P. H. Leo, J. S. Lowengrub, and H. J. Jou, A diffuse interface model for microstructural evolution in elastically stressed solids, *Acta Mater.*, **46** (1998), pp. 2113–2130.

[57] P. H. Leo and R. F. Sekerka, The effect of surface stress on crystal–melt and crystal–crystal equilibrium, *Acta Metall.*, **37** (1989), pp. 3119–3138.

[58] F.-H.Lin, Variational problems with free interfaces, *Calc. Var.*, **1** (1993), pp. 149-168.

[59] S. Luckhaus, The Stefan problem with the Gibbs-Thomson relation for the melting temperature, *European J. Appl. Math.*, **1** (1991), pp. 101-111.

[60] S. Luckhaus and L. Modica, The Gibbs-Thoson relation within the gradient theory of phase transitions, *Arch. Rat. Mech. Anal.*, **107** (1989), pp.71-83.

[61] S. Luckhaus and T. Sturzenhecker, Implicit time discretisation for the mean curvature flow equation, *Calc. Var.*, **3** (1995), pp. 253–271.

[62] M. Mahadevan and R. M. Bradley, Phase field model of surface electromigration in single crystal metal thin films, *Physica D* **126** (1999), pp. 201–213.

[63] S. Maier-Paape and T. Wanner, Spinodal decompositon for the Cahn-Hilliard equation in higher dimensions. Nonlinear dynamics, *Arch. Rat. Mech. Anal.*, **151** (2000), pp. 187-219.

[64] T. Merkle, An energy method for the strongly nonlinear Cahn-Larché equation system, Universität Stuttgart, IANS Preprint 2003/016.

[65] A. Miranville, Long-time behavior of some models of Cahn-Hilliard equations in deformable continua, *Nonlinear Anal. Real World Appl.* **2** (2001), no. 3, pp. 273–304.

[66] A. Miranville, Consistent models of Cahn-Hilliard-Gurtin equations with Neumann boundary conditions, *Phys. D* **158** (2001), no. 1-4, pp. 233–257.

[67] L. Modica, The gradient theory of phase transition and the minimal interface criterion, *Arch. Rat. Mech. Anal.*, **98** (1987), pp. 123-142.

[68] L. Modica and S. Mortola, Un esempio di Γ-convergenza, *Boll. Un. Mat. Ital.*, **5** 14-B (1977), pp. 285-299.

[69] S. Müller-Urbaniak, Eine Analyse des Zwischenschritt-θ-Verfahrens zur Lösung der instationären Navier-Stokes-Gleichungen, Preprint 94–01 des SFB 359 (1994).

[70] W. W. Mullins, Theory of thermal grooving, *J. Appl. Phys.* **28** (1957), pp. 333-339.

[71] A. Onuki, Ginzburg–Landau approach to elastic effects in the phase separation of solids, *J. Phys. Soc. Jpn.*, **58** (1989), pp. 3065–3068.

[72] R. L. Pego, Front migration in the nonlinear Cahn-Hilliard equation, *Proc. Roy. Soc. London Ser. A* **422** (1989), no. 1863, 261–278

[73] M. Röger, Existence of weak solutions for the Mullins-Sekerka flow, Preprint (2004).

[74] L. L. Shanahan and B. J. Spencer, A codimension-two free boundary problem for the equilibrium shapes of a small three-dimensional island in an epitaxially strained solid film, *Interfaces and Free Boundaries* **4** (2002), 1–25.

[75] B. J. Spencer, P.W. Voorhees, and S.H. Davis, Morphological instability in eptaxially strained dislocation-free solid films: Linear stability theory, *J. Appl. Physics* **73** (1993), 4955–4970.

[76] B. Stoth, Convergence of the Cahn-Hilliard equation to the Mullins-Sekerka problem in spherical symmetry, *J. Differential Equations* **125** (1996), no. 1, pp. 154–183.

[77] U. Weikard, Numerische Lösungen der Cahn-Hilliard-Gleichung und der Cahn-Larché-Gleichung, PhD thesis, Bonn (2002).